IEEE Access
Multidisciplinary | Rapid Review | Open Access Journal

Received October 13, 2016, accepted October 17, 2016, date of publication October 20, 2016, date of current version November 18, 2016.

Digital Object Identifier 10.1109/ACCESS.2016.2619379

Throughput Improvement in Cellular Networks via Full-Duplex Based Device-to-Device Communications

XIAOMENG CHAI[1], TONG LIU[2], CHENGWEN XING[3], HAILIN XIAO[4], AND ZHONGSHAN ZHANG[1]

[1]Beijing Engineering and Technology Center for Convergence Networks and Ubiquitous Services, University of Science and Technology Beijing, Beijing 100083, China
[2]Department of Information and Communication Engineering, Harbin Engineering University, Harbin 150001, China
[3]School of Information and Electronics, Beijing Institute of Technology, Beijing 100081, China
[4]Key Laboratory of Cognitive Radio and Information Processing, Ministry of Education, Guilin University of Electronic Technology, Guilin 541004, China

Corresponding author: Z. Zhang (zhangzs@ustb.edu.cn)

This work was supported in part by the key project of the National Natural Science Foundation of China under Grant 61431001, in part by the Key Laboratory of Cognitive Radio and Information Processing, Ministry of Education (Guilin University of Electronic Technology), and in part by the Foundation of Beijing Engineering and Technology Center for Convergence Networks and Ubiquitous Services.

ABSTRACT In this paper, throughput improvement of device-to-device (D2D)-aided underlaying cellular networks is analyzed. The D2D devices are assumed to be capable of operating at the full duplex (FD) mode to enable the concurrent transmission and reception with a single frequency band. We analyze the impact of activating D2D users on the throughput of FD-based D2D (FD-D2D) aided underlaying network by considering non-ideal self-interference cancellation at the FD devices. Despite of an extra interference imposed on the cellular users (CUs) by the active D2D links, which may erode the signal-to-interference ratio of the former significantly, the FD-D2D mode is still shown to exhibit its superiority in terms of the throughput improvement. Furthermore, in order to avoid a severe FD-D2D-induced interference imposed on the CUs, a new mechanism called "dynamic cellular link protection (DCLP)," which prohibits the transmissions of FD-D2D users when they are located inside the pre-set guard areas, is proposed. Numerical results show that the proposed DCLP mechanism is capable of substantially improving the throughput of the underlaying cellular networks without seriously eroding the capacity of the conventional cellular links.

INDEX TERMS Underlaying cellular network, device-to-device, full duplex, self-interference, throughput.

I. INTRODUCTION

With the rapid development of wireless communication techniques, the existed cellular networks are becoming increasingly difficult to meet the customers' exponentially growing data traffic demand [1]–[4]. Meanwhile, the base stations (BSs) (particularly that deployed in the hot spot areas) may often operate at an overloaded state due to the BS-centric architecture of the existed wireless access network (WAN), thus resulting in a serious load imbalance over the whole WAN [5].

To successfully relieve the above-mentioned issues, the Device-to-Device (D2D) technique, which allows the proximity users to communicate directly with each other (i.e. without relying on the intervention of BSs), has been proposed by reflecting several promising advantages, such as substantially enhancing the network's throughput [6] as well as spectral efficiency [7], extending the radio coverage of mobile users [8], saving the devices' power consumption [9] and effectively offloading the traffic from the BS side to the mobile terminal side [10], etc. Unlike the conventional cellular users (CUs) in the existed BS-centric WANs, the D2D peers are enabled to establish a direct link between them, thus substantially improving the signal-to-interference-plus-noise ratio (SINR) at the D2D receiver due to the mitigation of excessive power loss induced by large-scale fading.

Currently, D2D technique has attracted a wide attention in both academia and industry. In most of the existed studies, conventional half duplex (HD) mode has been overwhelmingly adopted [11]. Unlike the HD mode, the full duplex (FD) mode[1] enables a device to perform a concurrent transmission and reception in a single frequency band, thus (in theory)

[1]Although FD mode has long been regarded as impractical in the past due to the large power difference between the self-interference (SI) and the signal-of-interest received from a remote source [12], the latest SI cancellation techniques can be employed to effectively reduce the SI to a very low level [13].

improving the attainable spectral efficiency by a factor of two [13]–[15].

All the above-mentioned technical advantages have motivated us to investigate the combination of D2D communications and FD mode [11]. However, before we can successfully implement the FD based D2D (FD-D2D) technique, there still exist several challenges to address. For instance, to operate the practical D2D-based systems, the active D2D links may either occupy a dedicated resource (i.e. the resource that is orthogonal to the cellular bandwidth) [16] or reuse the CU's licensed resources [17]. Relative to the former resource-allocation scheme, the same spectrum will be shared between the DUs and the conventional CUs in the latter, thus (with a high possibility) causing a serious interference between CUs and DUs. Consequently, the interference-management techniques may constitute a major concern of D2D-enabled underlaying cellular networks. More importantly, as compared with the HD based D2D (HD-D2D) mode, the non-zero SI power may also significantly erode the performance of FD-D2D devices.

A. MOTIVATION

The interference-management techniques for D2D-aided cellular networks have been widely studied. Basically, the existing interference-management techniques can be divided into the following two categories: *mode selection* and *resource management* [18]. The *mode selection* based technique enables the mobile users to choose an appropriate operational mode from the two candidates, i.e. the conventional cellular mode and D2D. The *resource management* based technique, on the other hand, is capable of optimizing the network performance by properly allocating resources, such as power, time slots and radio spectrum, to the mobile users [19]. In each category, the interference imposed on the mobile users by the active D2D links may always erode the performance of the former. For instance, it could instantaneously impose a severe interference on the conventional CUs if the geographically close-by D2D links are being activated. Furthermore, the DU-to-DU interference may even deteriorate the performance gain of the whole D2D system.

Despite all this, the D2D technology still reveals a lot of technical advantages. In particular, FD-D2D technique is of a great potential in improving the throughput of the whole underlaying network due to the following reason: *In light of the fact that the D2D mode is essentially service-oriented and a D2D link can be created when and only when a service demand emerges between D2D peers, the mute duration of the D2D links (i.e. the D2D transmitter does not transmit) can still be regarded as the interference-free period from the perspective of conventional CUs.*[2] *From this point of view, it would be critical to complete a given D2D service (i.e. with a given amount of data to exchange between D2D peers) as quick as possible in order to minimize the impact of D2D-imposed interference.*

Intuitively speaking, an efficient and straightforward way of minimizing the impact of D2D-imposed interference on the conventional CUs might resort to the method of extending the D2D mute duration (i.e. corresponding to suppressing the active duration of D2D peers), provided that the given amount of data can be successfully exchanged between D2D peers. When we need to exchange a given amount of data between D2D peers, either HD or FD mode can be employed in the D2D communications. As compared to the former, the latter is (in theory) capable of doubling the data rate, corresponding to cutting the D2D-active period by half. Although the average interference level imposed on the CUs by the FD-D2D users becomes higher than that by the HD-D2D users, the accumulated performance losses due to the former are still expected to be lower than that induced by the latter, because the average data transmission duration (i.e. the D2D-induced interference period)[3] required in the latter is almost two times of that in the former. Obviously, it would be beneficial to improving the throughput of the D2D-aided cellular networks by employing FD mode rather than HD mode, because FD-D2D is shown to be helpful to substantially expediting the completion of D2D services for a given amount of data to be exchanged between D2D pairs.

B. RELATED WORKS

In order to alleviate the limitations observed in the conventional BS-centric WAN architecture in terms of constrained radio coverage and service-providing capability, the cellular networks with an integration of D2D mode has attracted a wide attention. In light of the fact that an additional interference will be imposed on the CUs by the active D2D links, an appropriate interference management technique (e.g. techniques of mode selection and resource allocation) may play a critical role in optimizing the performance of D2D-aided underlaying cellular networks. For instance, a mode selection scheme [20] can be carried out by estimating the achievable transmission probability of both the CUs and DUs, with the qualities of the D2D/cellular links under various interference situations considered. Furthermore, the sum-rate of the underlaying networks can be optimized by jointly performing mode selection and resource allocation techniques subject to the constraints of spectral efficiency and power consumption. Three link-sharing strategies, including *non-orthogonal sharing* mode, *orthogonal sharing* mode and *cellular* mode [21], are considered in the above-mentioned joint scheme. Moreover, to enhance the capacity of D2D-aided networks, authors in [22] proposed a new scheme to enable the CUs to be capable of reserving a part of their transmission power for performing the D2D mode. In addition, the authors in [23] formulated a joint-optimization problem by combining the schemes of mode selection, resource allocation and power allocation in a multi-cell network, in which a distributed sub-optimal heuristic algorithm can be employed for solving

[2]During the interference-free period, the D2D-induced interference imposed on the conventional CUs will instantaneously disappear.

[3]Note that a given amount of data is always assumed to be exchanged between HD/FD-D2D peers.

the NP-Hard problem encountered in the proposed joint-optimization scheme.

Despite all that, almost all the existing works overwhelmingly considered HD-D2D mode rather than FD-D2D mode. Basically, FD mode would be much more suitable for D2D communications than HD mode does due to its capability of doubling the spectral efficiency of WANs (provided that a proper SI cancellation scheme can be performed in the former so as to maintain a relatively weaker SI level at the FD-D2D devices). Recently, some preliminary studies on adopting FD mode in D2D communications have been carried out. For instance, an interference-suppression mechanism for FD-aided cellular networks is proposed in [24] by properly designing the transmitted signals for the D2D links. Furthermore, authors in [25] proposed an FD-relaying scheme to enable the operation of underlaying D2D-cellular networks. In addition, the throughput-maximization problem in FD-D2D mode has been formulated and solved by employing the schemes of resource sharing [26] and power allocation [27]. Last but not least, all the above-mentioned works have considered a relatively simple scenario (i.e. in most cases, a single-cell scenario containing only a single FD-D2D pair was considered). Basically, the spatially distributed BSs and CUs in practical scenarios would, to a large extent, impact the accumulated interference of the objective users. Furthermore, most of the existing works have considered only the sum-rate maximization of the underlaying networks, while lacking of the analysis on the critical issues that would significantly erode the quality of cellular links. Intuitively speaking, the DU density will play a critical role in impacting the performance of D2D-aided cellular networks [28].

Another important issue caused by employing D2D technology is the increased risk of upsetting the fairness among the users in terms of resource allocation priority. Compared with the cellular links, the D2D links are capable of offering a much higher data rate, thus making the system tend to tilt toward the DUs when allocating the resources. Consequently, the above-mentioned tendency may result in a significant traffic-load hungry in the conventional CUs, if the objective function of the underlaying network is simply set to be ''pursuing the sum-rate maximization''. To avoid the above-mentioned risk, a received signal strength (RSS) threshold based scheme has been proposed in [29] for preventing any user from activating the D2D mode if the RSS from the nearest BS is higher than a specified threshold. Furthermore, in [30], the authors proposed a new scheme to enable the data-rate maximization in the underlaying networks by guaranteeing the predefined service levels of the CUs in a distributed manner. However, the authors in [30] failed to derive the closed-form expressions for the performance indexes of coverage probability and data-rate.

C. MAIN CONTRIBUTIONS

In this paper, we investigate the performance gain in the underlaying networks by employing FD-D2D technique in the scenario of spatially distributed multiple cells, with the sum network throughput analyzed. A new scheme referred to as ''Dynamic Cellular Link Protection (DCLP)'' is proposed by considering the impact of the distance between the objective CU and its serving BS. The main contributions of this paper are reflected in the following three aspects:

1) Based on the theory of stochastic geometry, a new framework is established for modelling and analyzing the throughput of cellular/D2D links. Both the FD and the HD modes are considered in the new framework. Furthermore, we analyze the tight throughput bounds of the FD-D2D based underlaying network by deriving the closed-form expressions for those bounds. Although the FD-D2D mode may impose a higher interference on the mobile terminals than that imposed by the HD-D2D mode, the former still exhibits its superiority in terms of the sum throughput.
2) Although the sum throughput of underlaying network can be substantially improved by activating FD-D2D mode users, there always exists a break-even point in the attainable performance gain of the FD-D2D aided underlaying networks, beyond which the sum throughput cannot be further increased by simply increasing the density of DUs (i.e. because of the negative effect of overloaded interference on the sum throughput). The break-even point of the FD-D2D aided underlaying networks will be identified in this paper.
3) To guarantee the quality of conventional CUs, a DCLP mechanism is proposed to prevent the FD-D2D users from transmitting if they are located inside the pre-set guard areas. The radius of the guard area is parameterized by the distances between the objective CUs and their serving BS. By implementing the proposed DCLP mechanism, the signal-to-interference ratio (SIR) of the cell-edge CUs would not become intolerably low.

The remainder of this paper is organized as follows. In Section II, the system model for the proposed FD-D2D aided underlaying cellular networks is described. The theoretical analysis for the transmission rates in both the FD and the HD modes are provided in Section III, followed by proposing the DCLP mechanism in Section IV. Furthermore, numerical results are given out by Section V. Finally, Section VI concludes this paper.

Notation: $\mathbb{P}\{\bullet\}$ represents the probability of an event, and $\mathbb{E}\{\bullet\}$ denotes the expectation operation. $\mathcal{S}_{\{\bullet\}}$ stands for the successful transmission probability of a wireless communications link, and $T\{\bullet\}$ represents the throughput of a wireless communications link. Furthermore, $\mathcal{L}\{\bullet\}$ denotes the Laplace transforms of a random variable.

II. UPLINK SYSTEM MODEL FOR FD-D2D BASED UNDERLAYING CELLULAR NETWORKS

In this paper, a cellular system comprising multiple BSs and mobile user equipments (UEs) is considered. The proposed system model in terms of network architecture, communication link modelling and interference analysis is given out in the following subsections.

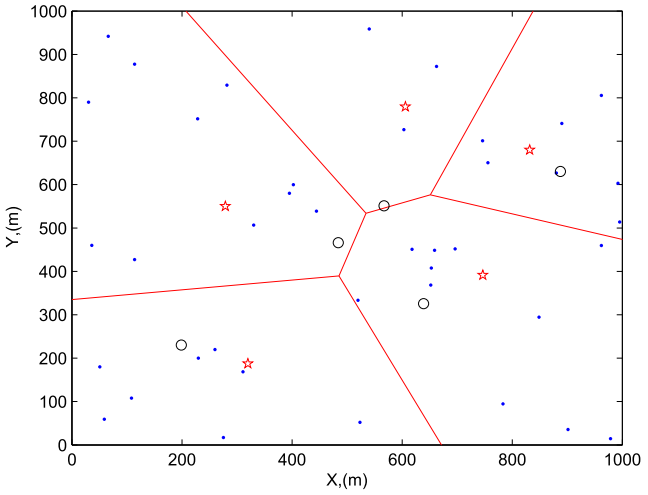

FIGURE 1. The general D2D aided underlaying cellular network with Poisson-Voronoi cell tessellation. The red asterisks represent the BSs, and the circles and points represent the CUs and DUs, respectively.

A. NETWORK ARCHITECTURE OF THE PROPOSED UNDERLAYING NETWORKS

In this section, we assume that the BSs and the conventional CUs are spatially distributed within a given geographical area according to the models of classical homogeneous Poisson point process (PPP)[4] Φ_b and Φ_c of intensities λ_b and λ_c, respectively. Without loss of generality, orthogonal resource allocation is assumed to be performed among co-BS CUs for effectively mitigating the intra-cell interference. Furthermore, the DUs are assumed to be geographically scattered within the cellular coverage according to an independently marked PPP $\hat{\Phi}_d = \{x_i, m(x_i)\}$, where the ground process $\Phi_d = \{x_i\}$ with intensity λ_d represents the location of one side of the (FD mode) D2D pair, and the marked process $\{m(x_i)\}$ represents the other side of the D2D pair that x_i communicates with. In addition, we assume that the correspondent FD-DU is randomly distributed around its D2D peer with an average distance D_d, implying that $\|x_i - m(x_i)\| = D_d$ and $m(x_i) = x_i + D_d(\cos\varphi_i, \sin\varphi_i)$ are satisfied, where the parameters φ_i are assumed to be independently and uniformly distributed (i.i.d.) in $[0, 2\pi)$. In Fig. 1, we illustrate an example of the Poisson-Voronoi cell tessellation, with the red asterisks representing the BSs, while the circles and points denoting CUs and DUs, respectively.

B. SIR ANALYSIS FOR BOTH THE CELLULAR AND D2D LINKS

We consider an FD-D2D aided underlaying cellular network, in which the conventional cellular links are assumed to be operated at the HD mode, while the D2D links are operated at the FD mode. According to the existing standards such as ProSe [32], the cellular network's uplink resources are reused for implementing the D2D communications. Without loss of generality, orthogonal resource allocation is assumed to be performed among co-BS CUs.

To model the cellular/D2D links as well as the interference links, both the large-scale power law propagation model and the small-scale (e.g. Rayleigh fading) model are taken into account. Particularly, by considering the transmitter-to-receiver distance d and transmit power p, the signal power received at a receiver can be denoted by $s = p \cdot h_{ij} \cdot d^{-\alpha}$, where h_{ij} stands for the exponentially distributed fading coefficient between the transmitter i and the receiver j (i.e. Rayleigh fading is assumed), and α represents the standard path loss exponent subject to constraint $\alpha > 2$. Furthermore, the i.i.d. links are assumed in the above-mentioned model, corresponding to $h_{ij} \sim \exp(1)$, $i, j \in \{\Phi_b, \Phi_c, \Phi_d\}$.

In the following, a constant transmit power is assumed in each UE, with P_c and P_d denoting the transmit power of CUs and DUs, respectively. The received SIR of a typical cellular link and a D2D link can be expressed as

$$\mathrm{SIR}_c = \frac{P_c h_{cb} d_{cb}^{-\alpha}}{I_{dc} + I_{cc}}, \tag{1}$$

$$\mathrm{SIR}_d = \frac{P_d h_d D_d^{-\alpha}}{I_{cd} + I_{dd} + I_{SI}}, \tag{2}$$

respectively, where $I_{dc} = \sum_{x_i \in \Phi_d} (P_d h_{x_i b} d_{x_i b}^{-\alpha} + P_d h_{m(x_i)b} d_{m(x_i)b}^{-\alpha})$ denotes the interference power imposed on CUs by FD-mode DUs, $I_{dd} = \sum_{x_i \in \Phi_d / x_d} \left(P_d h_{x_i d} d_{x_i d}^{-\alpha} + P_d h_{m(x_i)d} d_{m(x_i)d}^{-\alpha} \right)$ stands for the inter-DU interference, $I_{cc} = \sum_{c_i \in \Phi_c / c_0} P_c h_{c_i b} r_{c_i b}^{-\alpha}$ represents the interference among CUs, $I_{cd} = \sum_{c_i \in \Phi_c} P_c h_{c_i d} r_{c_i d}^{-\alpha}$ stands for the interference power imposed on DUs by CUs, $I_{SI} = P_d / c_{si}$ denotes the residual SI observed in the FD devices after performing SI cancellation,[5] and c_{si} denotes the SI cancellation coefficient (i.e. a larger coefficient implies a higher SI cancellation capability).

C. SUCCESSFUL TRANSMISSION PROBABILITY OF THE WIRELESS LINKS

We define the successful transmission probability (STP) of a cellular/D2D link as *the probability that the quality of a randomly chosen link successfully reaches its predetermined target SIR threshold* ε, as represented by

$$\mathcal{S}_c = \Pr\left(\frac{P_c h_{cb} d_{cb}^{-\alpha}}{I_{dc} + I_{cc}} > \varepsilon \right), \quad \text{Cellular Link}, \tag{3}$$

$$\mathcal{S}_d = \Pr\left(\frac{P_d h_d D_d^{-\alpha}}{I_{cd} + I_{dd} + I_{SI}} > \varepsilon \right), \quad \text{D2D Link}, \tag{4}$$

[4]Note that in the practical environment, the BSs' distributions are different from the standard PPP, and the Poisson-Voronoi cell tessellation can only serve as an approximation of the actual cellular cells, because the BSs' locations are usually carefully planned by the operators rather than randomly distributed according to the principle of random process. The main reason for us to adopt the PPP model in this paper is to keep the analysis tractable. In fact, PPP distribution can be considered as a worst-case scenario of the cellular systems. The excellent properties of PPP make it tractable of capturing the major random features of cellular system and deriving the closed-form expressions of some performance indicators such as SIR distribution [31].

[5]Many existing SI cancellation techniques can be employed for reducing the SI power to a very low level. However, SI cancellation is beyond the scope of this paper. The interested readers may refer to [13] for details.

respectively. Note that STP here is equivalent to the concept "coverage probability" that defined in some other literatures [33].

III. THROUGHPUT FOR FD-D2D BASED UNDERLAYING CELLULAR NETWORKS

In this section, the theory of stochastic geometry is employed for modelling and analyzing the throughput of the proposed underlaying system. Specifically, the throughput of FD-D2D based underlaying cellular networks in the presence of non-zero residual SI power will be analyzed.

A. STP OF A TYPICAL LINK

From the Slivnyakąś theorem [34], the statistical property of a typical node located at a specific position holds true for any generic node located at any generic location. Without loss of generality, we assume that the node of interest is located at the origin of the plane.

- For a typical cellular link, the STP can be represented as

$$\mathcal{S}_c^f = \int_0^\infty \mathcal{L}_{I_{cc}}\left(\frac{\varepsilon r^\alpha}{P_c}\right)\mathcal{L}_{I_{dc}}\left(\frac{\varepsilon r^\alpha}{P_c}\right)e^{-\lambda_b \pi r^2} 2\pi\lambda_b r \mathrm{d}r, \tag{5}$$

  where $\mathcal{L}_{I_{cc}}(s)$ and $\mathcal{L}_{I_{dc}}(s)$ denote the Laplace transforms (evaluated at s) of random variables I_{cc} and I_{dc}, respectively, as given by

$$\mathcal{L}_{I_{cc}}(s) = \exp\left[-\pi\lambda_b r^2 \rho(\varepsilon,\alpha)\right] \tag{6}$$

$$\mathcal{L}_{I_{dc}}(s) = \exp\left[-\lambda_d \int_0^\infty \left(2\pi - \frac{f(s,D_d,\alpha)}{1+P_d s x^{-\alpha}}\right) x \mathrm{d}x\right], \tag{7}$$

  respectively, where $\rho(\varepsilon,\alpha) = \varepsilon^{\frac{2}{\alpha}} \int_{\varepsilon^{-\frac{2}{\alpha}}}^\infty \frac{1}{1+x^{\frac{\alpha}{2}}}\mathrm{d}x$ and $f(s,D_d,\alpha) = \int_0^{2\pi} \frac{1}{1+P_d s(x^2+D_d^2+2xD_d\cos\varphi)^{-\alpha/2}}\mathrm{d}\varphi$.
- For a typical FD-D2D link, the STP is represented as

$$\mathcal{S}_d^f = \mathcal{L}_{I_{cd}}\left(\frac{\varepsilon D_d^\alpha}{P_d}\right)\mathcal{L}_{I_{dd}}\left(\frac{\varepsilon D_d^\alpha}{P_d}\right)e^{-\varepsilon c_{si} D_d^\alpha}, \tag{8}$$

  where $\mathcal{L}_{I_{cd}}(s)$ and $\mathcal{L}_{I_{dd}}(s)$ are given by

$$\mathcal{L}_{I_{cd}}(s) = \exp\left[-\pi\lambda_b D_d^2 \left(\frac{P_d}{P_c}\right)^{2/\alpha}\delta(\varepsilon,\alpha)\right] \tag{9}$$

$$\mathcal{L}_{I_{dd}}(s) = \exp\left[-\lambda_d \int_0^\infty \left(2\pi - \frac{f(s,D_d,\alpha)}{1+P_d s x^{-\alpha}}\right) x \mathrm{d}x\right], \tag{10}$$

  respectively, with $\delta(\varepsilon,\alpha) = \dfrac{2\pi\varepsilon^{2/\alpha}}{\alpha\sin(2\pi/\alpha)}$.

The Proof of above-mentioned derivations are given out in Appendix A.

Since the closed-form expression for the STP of a typical link is hard to derive, if not impossible, the tight bounds for the STP will be employed instead.

Lemma 1: The STP of a typical cellular link $\mathcal{S}_c^f$ is lower and upper bounded by

$$\underline{\mathcal{S}}_c^f = \frac{1}{1+\rho(\varepsilon,\alpha)+2\frac{\lambda_d}{\lambda_b}\left(\frac{P_d}{P_c}\right)^{2/\alpha}\delta(\varepsilon,\alpha)}, \tag{11}$$

$$\overline{\mathcal{S}}_c^f = \frac{1}{1+\rho(\varepsilon,\alpha)+\left(1+\frac{2}{\alpha}\right)\frac{\lambda_d}{\lambda_b}\left(\frac{P_d}{P_c}\right)^{2/\alpha}\delta(\varepsilon,\alpha)}, \tag{12}$$

respectively. The proof of **Lemma 1** is provided in Appendix B.

Lemma 2: The STP of a typical D2D link $\mathcal{S}_d^f$ is lower and upper bounded by

$$\underline{\mathcal{S}}_d^f = \exp\left[-\pi D_d^2\left(\lambda_b\left(\frac{P_c}{P_d}\right)^{\frac{2}{\alpha}} + 2\lambda_d\right)\delta(\varepsilon,\alpha) - \frac{\varepsilon D_d^\alpha}{c_{si}}\right], \tag{13}$$

$$\overline{\mathcal{S}}_d^f = \exp\left[-\pi D_d^2\left(\lambda_b\left(\frac{P_c}{P_d}\right)^{\frac{2}{\alpha}} + \left(1+\frac{2}{\alpha}\right)\lambda_d\right)\delta(\varepsilon,\alpha) - \frac{\varepsilon D_d^\alpha}{c_{si}}\right], \tag{14}$$

respectively. The proof of **Lemma 2** is similar to that of **Lemma 1**.

B. THROUGHPUT ANALYSIS OF THE FD-D2D AIDED UNDERLAYING CELLULAR NETWORKS

One of the purposes of implementing the FD-D2D aided underlaying networks is to increase the sum throughput of the whole network. While the throughput of a D2D link can be increased by employing FD-D2D technique, an additional D2D-induced interference may be imposed on the geographically close-by UEs. In this subsection, we investigate the throughput of the FD-D2D aided underlaying cellular networks and analyze the attainable throughput gain in FD-D2D over HD-D2D.

First, let us define the sum throughput of a network as $T = \lambda\mathcal{S}\log(1+\varepsilon)$, where λ denotes the density of nodes, $\mathcal{S}$ represents the STP of a typical link and ε stands for the SIR. From the above-mentioned definitions, the sum throughput of the FD-D2D aided underlaying cellular network can be given by

$$T_f = \left(\lambda_b\mathcal{S}_c^f + 2\lambda_d\mathcal{S}_d^f\right)\log(1+\varepsilon). \tag{15}$$

Lemma 3: In the FD-D2D aided underlaying cellular networks, the optimal density of DUs in terms of the sum throughput is $\lambda_d^* = \dfrac{1}{\int_0^\infty\left(2\pi - \frac{f(s,D_d,\alpha)}{1+P_d s x^{-\alpha}}\right)x\mathrm{d}x}$, which is bounded by $\dfrac{1}{2\pi D_d^2\delta(\varepsilon,\alpha)} \le \lambda_d^* \le \dfrac{1}{\left(1+\frac{2}{\alpha}\right)\pi D_d^2\delta(\varepsilon,\alpha)}$.

Proof: Since the density of DUs is usually much higher than that of the BSs in underlaying networks, the throughput of the underlaying networks can be approximated as $T_f \approx 2\lambda_d\mathcal{S}_d^f\log(1+\varepsilon)$. Evidently, T_f is a convex function of λ_d,

leading to a straightforward proof of **Lemma 3** by making the partial derivative of $\overline{T_f} = \left(\lambda_b \overline{\mathcal{S}_c^f} + 2\lambda_d \overline{\mathcal{S}_d^f}\right) \log(1+\varepsilon)$ and $\underline{T_f} = \left(\lambda_b \underline{\mathcal{S}_c^f} + 2\lambda_d \underline{\mathcal{S}_d^f}\right) \log(1+\varepsilon)$ in terms of λ_d and letting the result equal 0. ■

Lemma 3 leads to the following observation: *when the density of DUs is relatively low, the throughput of the network can always be enhanced by increasing the number of DUs until a break-even point is approached (i.e. beyond which point the performance gain cannot be further increased, and the sum throughput will be eroded by further increasing the number of DUs).* We can explain this observation as follows: When the density of DUs becomes extremely high (i.e. beyond the break-even point), the cellular systems will become interference-overwhelmed, making the performance gain brought about by increasing the DUs be unable to counter-balance the capacity loss induced by the rapidly increased interference.

In order to evaluate the advantages of the FD-D2D technique with respect to the HD-D2D in terms of sum throughput gain, as a benchmark, we first derive the STP of a typical cellular and D2D link in HD-D2D aided underlaying cellular network as

$$\mathcal{S}_c^h = \frac{1}{1+\rho(\varepsilon,\alpha)+\frac{\lambda_d}{\lambda_b}\left(\frac{P_d}{P_c}\right)^{2/\alpha}\delta(\varepsilon,\alpha)}, \quad (cellular) \tag{16}$$

$$\mathcal{S}_d^h = \exp\left[-\pi D_d^2\left(\lambda_b\left(\frac{P_c}{P_d}\right)^{\frac{2}{\alpha}}+\lambda_d\right)\delta(\varepsilon,\alpha)\right], (D2D) \tag{17}$$

respectively.

Lemma 4: The throughput gain brought about by employing the FD-D2D mode with respective to the HD-D2D mode can be derived as

$$2\exp\left(-\pi D_d^2\lambda_d\delta(\varepsilon,\alpha)-\varepsilon D_d^\alpha/c_{si}\right) \le \frac{T_f}{T_h} \le 2\exp\left(-\frac{2}{\alpha}\pi D_d^2\lambda_d\delta(\varepsilon,\alpha)-\varepsilon D_d^\alpha/c_{si}\right), \tag{18}$$

Meanwhile, in order to guarantee the FD-D2D technique to obtain the advantage of HD-D2D technique in terms of sum throughput, the amount of SI cancellation must satisfy the condition of $c_{\mathrm{si}} \ge \frac{\varepsilon D_d^\alpha}{\ln 2 - \pi D_d^2\lambda_d\delta(\varepsilon,\alpha)}$.

Proof: The throughput of the HD-D2D underlaying network can be approximated as $T_h = (\lambda_b\mathcal{S}_c^h + \lambda_d\mathcal{S}_d^h)\log(1+\varepsilon) \approx \lambda_d\mathcal{S}_d^h\log(1+\varepsilon)$. The proof of **Lemma 4** can be straightforwardly obtained by making the minimum of T_f/T_h to be larger than 1, as given by $2\exp\left(-\pi D_d^2\lambda_d\delta(\varepsilon,\alpha)-\varepsilon D_d^\alpha/c_{si}\right) \ge 1$ ■

Evidently, the superiority of FD-D2D over HD-D2D in terms of sum throughput mainly comes from the essential of concurrent transmission and reception at the former, corresponding to the factor-2 gain reflected in the throughput formula. However, this factor-2 gain is not fully attainable in practical designs mainly due to the performance erosion induced by the residual SI in FD devices. If, on the other hand, the amount of SI cancellation is less than $\frac{\varepsilon D_d^\alpha}{\ln 2 - \pi D_d^2\lambda_d\delta(\varepsilon,\alpha)}$, the HD-D2D mode may occasionally outperform the FD-D2D mode.

Here we need to emphasize that the above-mentioned (theoreticalčl' factor-2 gain is completely determined based on the physical-layer FD gain. In addition to the essential physical-layer gain of FD mode, the characteristic of services in practical systems will also have an impact on the FD-D2D gain. In practical systems that enable the D2D mode, a pair of D2D peers usually create the D2D link between them once there comes an amount of data to be exchanged between them, and this D2D link will be immediately removed if the data exchange is completed (i.e. for the purpose of releasing the occupied spectrum resources). In other words, D2D mode is essentially service-oriented and an active D2D link is maintained when and only when a service demand emerges between a pair of D2D peers. For a given amount of data to be exchanged between a pair of D2D peers, employing FD-D2D corresponds to shortening the D2D-imposed interference period to half of that by employing HD-D2D, because the FD mode is (in theory) capable of achieving two times the data rate of the latter under the same bandwidth utilization. Although the instantaneous interference level imposed on the CUs by the active FD-D2D links (during the data exchange period) is higher than that imposed by the active HD-D2D links, the FD-D2D induced interference can be quickly terminated as compared to the HD-D2D mode, provided that the D2D links will be removed immediately after the data-exchange process being completed. From this point of view, for a given block of data to be exchanged between D2D pairs, FD-D2D is helpful to substantially expediting the completion of D2D services, as shown in Fig.7. Since a relatively longer interference-free period is expected to be obtained by employing FD-D2D, it has always been able to gain the advantage with respect to HD-D2D mode in terms of sum throughput.

IV. DYNAMIC CELLULAR LINK PROTECTION MECHANISM

As analyzed in Section III, the interference-period-expediting effect observed in employing FD-D2D mode is beneficial to improving the sum network throughput from a statistics perspective. However, as the density of DUs increases, the conventional CUs may fail to communicate with their serving BSs due to the impact of severe D2D-induced interference. In this case, the throughput of the conventional CUs is eroded to some extent. In order to mitigate the above-mentioned performance erosion in CUs, we may offer the conventional CUs a higher priority than the DUs in terms of wireless resource allocation. To this end, a new resource allocation mechanism referred to as "DCLP" is proposed for preventing the FD-D2D users from guard range.

A. THE PRINCIPLE OF THE DCLP MECHANISM

Recall that the FD-D2D pairs will reuse the cellular's licensed spectrum,[6] the interference imposed on the cellular uplink by the active D2D pairs can be formulated as a function of the DU-to-BS distance. Evidently, this kind of D2D-induced interference can be reduced by keeping DUs away from BS. For the sake of guaranteeing the quality of cellular links, a new concept referred to as "guard area" from the perspective of cellular links (or in other words, "restricted zones" in terms of D2D links) can be defined as *a BS-centered geographical area with radius $R_p = k \cdot r$, where k is the DCLP coefficient and r denotes the distance between CU and BS. Within this guard area, the D2D transmitters must keep silent*.

For further explaining the concept of "guard area", it does not mean that the DUs in the guard area of interest will definitely be deactivated under all resource-allocation conditions. Note that the resource occupied by the CUs are orthogonal to each other, and the guard areas of different CUs usually do not overlap with each other. As long as the DUs' spectrum does not collide with any CU associated with the objective guard area, the DUs inside this objective guard area can still be activated.

When we define the range of "guard area (i.e. restricted zones)", the variation of cellular links' quality should be taken into consideration. In other words, the guard area is a dynamic rather than static function of the average length of cellular links. The dynamic essence of the cellular links enables the creation of D2D links by considering the following scenarios:

- When a relatively higher quality of the cellular links can be obtained (i.e. the CUs are geographically closed to the BSs), a more relieved constraint on the creation of FD-D2D links is permitted, corresponding to defining a relatively smaller "guard area". In this case, the FD-D2D links may lead to a substantial improvement in terms of the sum network throughput;
- When the cellular links have a relatively lower quality (i.e. the CUs are far away from the BSs), a relatively wider "guard area" will be determined to prohibit the creation of FD-D2D links inside this area. This extended "guard area" will substantially decrease the D2D-imposed interference on CUs.

B. STP ANALYSIS UNDER THE DCLP MECHANISM

In light of the fact that the DCLP mechanism does not influence the distribution of CUs, the parameters $\mathcal{L}_{I_{cc}}$ and $\mathcal{L}_{I_{cd}}$ defined above will not be modified under DCLP. In this case, the only parameters we need to modify will be I^n_{dc} and I^n_{dd}. Under the DCPL mechanism, the distribution of DUs no longer follows a standard PPP. Instead, a Poisson Hole Process (PHP) is employed for better modelling this probability distribution [35].

[6]For example, as specified in the existing standard ProSe [32], the licensed uplink spectrum will be reused by the DUs.

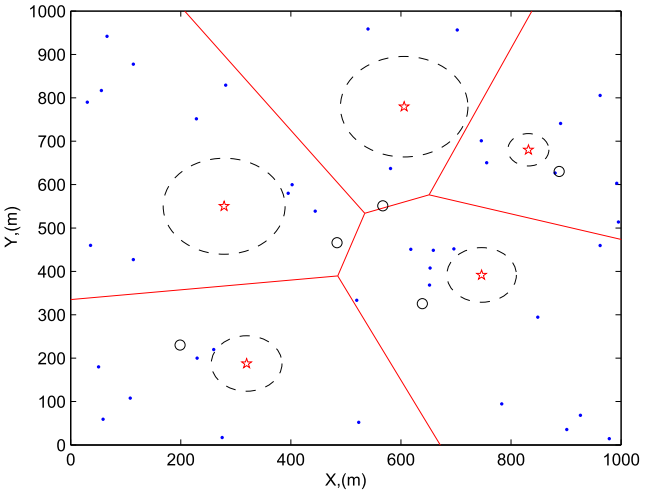

FIGURE 2. Illustration of D2D aided cellular network under DCLP mechanism, with the dotted circles representing the guard areas for the cellular links.

From Appendix C, $\mathcal{L}_{I^n_{dc}}$ and $\mathcal{L}_{I^n_{dd}}$ can be derived as

$$\mathcal{L}^n_{I_{dc}}(s) = \exp\left[-\lambda_d \int_{kr}^{\infty} \left(2\pi - \frac{f(s, D_d, \alpha)}{1 + P_d s x^{-\alpha}}\right) x \mathrm{d}x\right] \times \exp\left[-2\pi\lambda_b \int_{kr}^{\infty} \left(1 - e^{g(v,s)}\right) v \mathrm{d}v\right], \quad (19)$$

$$\mathcal{L}^n_{I_{dd}}(s) = \exp\left[-\lambda_d \int_{0}^{\infty} \left(2\pi - \frac{f(s, D_d, \alpha)}{1 + P_d s x^{-\alpha}}\right) x \mathrm{d}x\right] \times \exp\left[-2\pi\lambda_b \int_{0}^{\infty} \left(1 - e^{g(v,s)}\right) v \mathrm{d}v\right], \quad (20)$$

respectively, where $g(v, s) = \int_{v-kr}^{v+kr} 2\lambda_d \left(1 - \frac{f(s,D_d,\alpha)}{1+P_d s x^{-\alpha}}\right) \arccos\left(\frac{x^2+\|b_i\|^2-k^2r^2}{2\|b_i\|x}\right) x \mathrm{d}x$. Note that the main difference between $\mathcal{L}_{I^n_{dc}}$ and $\mathcal{L}^n_{I_{dd}}$ is reflected at the domain of the integration. Specifically, for a typical cellular link, the receiver of interest (i.e. BS) is located inside the nearest hole, which is totaly different from the case of a typical D2D link, in which the receiver of interest (i.e. DU) does not locate inside any holes.

By taking (19) and (19) into (5), (8) and (15), the STP under DCLP mechanism can be obtained. However, a closed-form expression for STP is still hard to obtain, if not impossible. For succinct, we derive the tight approximation for it. Note that the contribution of geographically close-by holes on the STP is much higher than that contributed by the holes located farther away due to the impact of path-loss effect. Therefore, we consider only the close-by holes by ignoring the impact of the holes of longer distance. Obviously, an approximation error lower than the actual value will appear due to the ignorance of holes of lower weights. As a compensation, we adopt the upper bound of the STP to correct it.

Lemma 5: The STP of cellular and D2D link under the DCLP mechanism can be approximated as

$$\mathcal{S}_c^n \approx \frac{1}{1+\rho(\varepsilon,\alpha)+\left(1+\frac{2}{\alpha}\right)\frac{\lambda_d}{\lambda_b}\left(\frac{P_d}{P_c}\right)^{\frac{2}{\alpha}}\rho_k(\varepsilon,\alpha,k)}, \quad (21)$$

and

$$\mathcal{S}_d^n \approx \exp\left[-\pi D_d^2\left(\lambda_b\left(\frac{P_c}{P_d}\right)^{\frac{2}{\alpha}}+\lambda_d\left(1+\frac{2}{\alpha}\right)\right)\delta(\varepsilon,\alpha)-\frac{\varepsilon D_d^\alpha}{c_{si}}\right], \quad (22)$$

respectively, where $\rho_k(\varepsilon,\alpha,k)=\varepsilon^{\frac{2}{\alpha}}\int_{\left(\frac{P_d\varepsilon}{P_c}\right)^{-2/\alpha}k^2}\frac{1}{1+x^{2/\alpha}}\mathrm{d}x$.

The tightness of the above-mentioned approximation will be evaluated relying on numerical analysis.

C. THE THROUGHPUT OPTIMIZATION OF DCLP COEFFICIENT

Basically, the proposed DCLP mechanism constitute a tradeoff between the quality of cellular links and the sum throughput of the network: *Compared with the conventional cellular links, the FD-D2D links are capable of contributing a higher percentage of the network throughput relying on their essential capabilities of simultaneously reducing the transmission power and shortening the communication distances. However, the above-mentioned situation may consequently lead to an imbalance of resource allocation between the cellular links and the D2D links, i.e. the resource will inevitably be tilted toward the DUs. This imbalance will inevitably erode the throughput of the cellular links.*

In order to mitigate the above-mentioned issue, the proposed DCLP mechanism must be capable of guaranteeing the minimum quality of cellular links. Under the DCPL mechanism, we can use $\tilde{\lambda}_d=\lambda_d\left(1-\lambda_b\int_0^\infty \pi k^2 r^2 x^{-\pi r^2\lambda_b}2\pi\lambda_b r\mathrm{d}r\right)=\lambda_d(1-k^2)$ to denote the equivalent density of DUs. The throughput under DCLP mechanism can thus be represented as $T_{DCLP}=\lambda_b\mathcal{S}_b+2\lambda_d(1-k^2)\mathcal{S}_d$. The throughput-maximization problem under DCLP mechanism can thus be formulated as

$$\begin{aligned}&\max_k\ T_{DCLP}=\lambda_b\mathcal{S}_c(k)+2\lambda_d(1-k^2)\mathcal{S}_d\\&s.t.\ O_c(k)\le\gamma,\end{aligned} \quad (23)$$

where $O_c(k)=1-\mathcal{S}_c(k)$ denotes the outage probability of cellular link (i.e. corresponds to the complement of STP). It is straightforwardly observed that T_{DCLP} and $O_c(k)$ are both monotonically decreasing functions of k, thus giving out the optimal DCLP coefficient as $k^*=O_c^{-1}(\gamma)$. For a given realization of α (e.g. $\alpha=4$), k^* can be obtained as

$$k^*=\sqrt{\frac{\sqrt{\frac{2P_d\varepsilon}{P_c}}}{\tan\left(\frac{\lambda_b}{\lambda_d}\sqrt{\frac{P_b}{2P_d}}\left[\frac{1-\gamma}{\gamma\sqrt{\varepsilon}}-\arctan(\sqrt{\varepsilon})\right]\right)}}. \quad (24)$$

V. NUMERICAL RESULTS

In this section, we first evaluate the performance gain in terms of throughput offered by employing FD-D2D mode in underlaying cellular networks, followed by exploring the benefits brought about by implementing the proposed DCLP mechanism on the cellular links' performance. Without loss of generality, the licensed uplink band is reused by the DUs, with i.i.d. Rayleigh fading channels considered in each link. Furthermore, the path-loss exponent α is set to 4 (i.e. corresponding to the typical urban environment).

In the following simulations, an objective environment with area $1000\times 1000m^2$, within which both BSs and DUs (with density of $5*10^{-6}$ and 10^{-4}, respectively) can be served. Furthermore, an orthogonal resource allocation among CUs is assumed, thus requiring the average number of instantaneous active CUs per cell to be 1. In addition, the average length of D2D links is assumed to be 30 m, with the transmit powers of CUs and DUs assumed to be 24 dBm and 20 dBm, respectively. The detailed parameter settings are shown in Table 1.

TABLE 1. Default key parameters in the simulation.

Parameter	Physical Meaning	Value
P_c	Power of CU	24 dBm
P_d	Power of DU	20 dBm
α	Path loss coefficient	4
D_d	The average distance between D2D peers	30 m
λ_b	Density of BS	5×10^{-6}
λ_d	Density of D2D link	10^{-4}
c_{si}	SI cancellation coefficient	80 dB

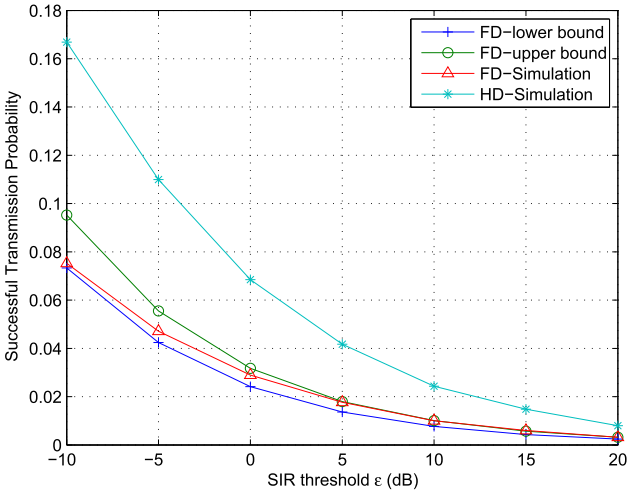

FIGURE 3. Performance comparison between FD-D2D under 80 dB SI cancellation and HD-D2D in terms of cellular link STP.

A. BENEFITS IN TERMS OF THROUGHPUT BROUGHT ABOUT BY FD-D2D

In this subsection, the performance comparison between the FD-D2D and conventional HD mode in terms of STP and throughput are performed. As shown in Fig. 3 and Fig. 4,

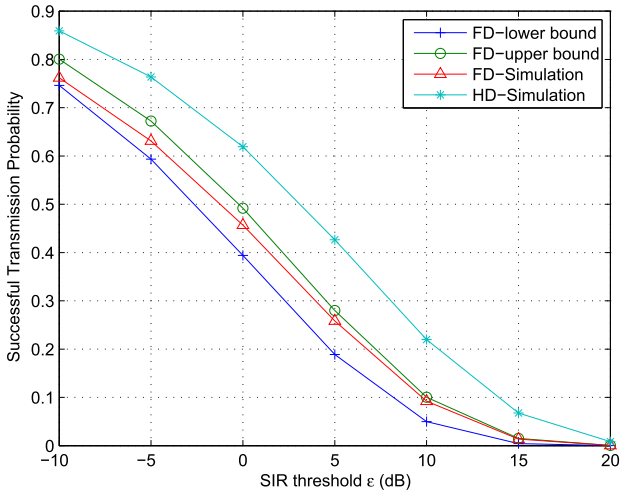

FIGURE 4. Performance comparison between FD-D2D under 80 dB SI cancellation and HD-D2D in terms of D2D link STP.

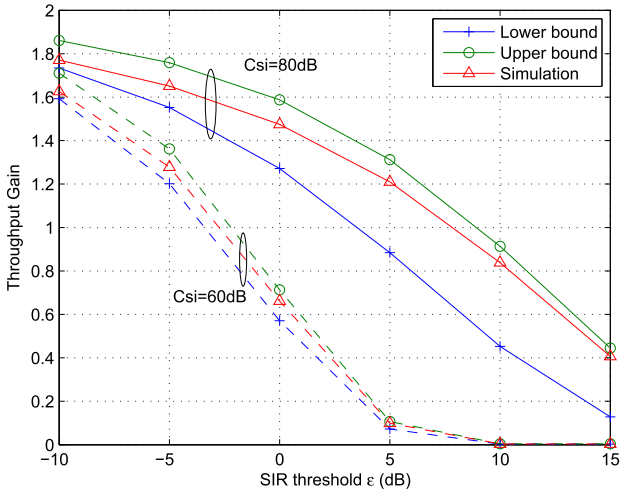

FIGURE 5. Throughput gain obtained by employing the FD-D2D mode than employing the HD-D2D mode by considering variant SI cancellation capabilities.

the theoretical STP bounds of both cellular and D2D links are tight enough. As compared to the HD-D2D aided networks, both the cellular and D2D links suffer from a higher D2D-induced interference by employing the FD-D2D mode, thus leading to a remarkable STP loss in both links. In Fig. 5, it evaluates the throughput gain brought about by employing FD-D2D under a variety of SI cancellation levels. As long as the SI cancellation capability is no higher than 60 dB, the throughput gain in most cases will be less than 1, implying that the HD-D2D mode outperforms the FD-D2D mode in terms of throughput. However, the FD-D2D mode exhibits its superiority in terms of the throughput if the SI-cancellation capability approaches 80 dB.

In Fig. 6, it illustrates the performance comparison between HD-D2D and FD-D2D modes in terms of throughput under various D2D densities. Evidently, the throughput can be improved as the D2D density increases. However, the way of improving the spectral efficiency by unlimitedly

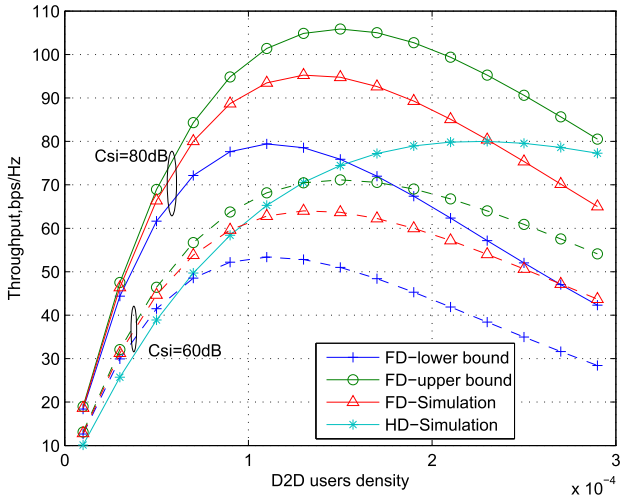

FIGURE 6. Performance comparison between HD-D2D and FD-D2D in terms of throughput under different D2D-density settings.

increasing the number of D2D links is shown to be not sustainable. As a result, the throughput may be eroded by further increasing the DUs density (i.e. beyond a critical break-even point). We may explain it as follows: In scenarios of sparse D2D distributions, activating more D2D pairs implies contributing more throughput via D2D links. With dense D2D distributions, on the other hand, the whole system becomes interference-overloaded, in which case the performance improvement brought about by increasing D2D pairs cannot counter-balance the throughput losses induced by the severe interference imposed by D2D links. Furthermore, as indicated by Fig. 6, the lower bound of maximum throughput obtained by employing the FD-D2D mode is almost equal to that obtained by employing the HD-D2D mode, with the optimal DUs density of the former being nearly half that of the latter. This is because the lower bound of interference imposed on the FD-D2D nodes comprise two dependent PPPs, which can be treated by using two independent PPPs with the same density, corresponding to creating a (summed) PPP with twofold density.

In Fig. 7, the performance gains brought about by employing HD-D2D and FD-D2D modes in terms of the average link spectral efficiency are compared. To be fair in comparison, a fixed-size block of data will be exchanged between each pair of D2D peers during their D2D-activate period. In spite of the fact that the above-mentioned case may not always happen in practical situations, it would still be regarded as a very typical scenario that a D2D link between two D2D peers will be created once the D2D peers have data blocks to share. In other words, the D2D links are activated in a service-driving manner. Note that the D2D links will be immediately closed after the data exchange is completed in order to mitigate the D2D-induced interference on the neighboring CUs/DUs. Furthermore, it is straightforward to conclude that the conventional CUs will suffer from a much more severe interference in the presence of geographically close-by activating FD-D2D links (i.e. due to the fact that the

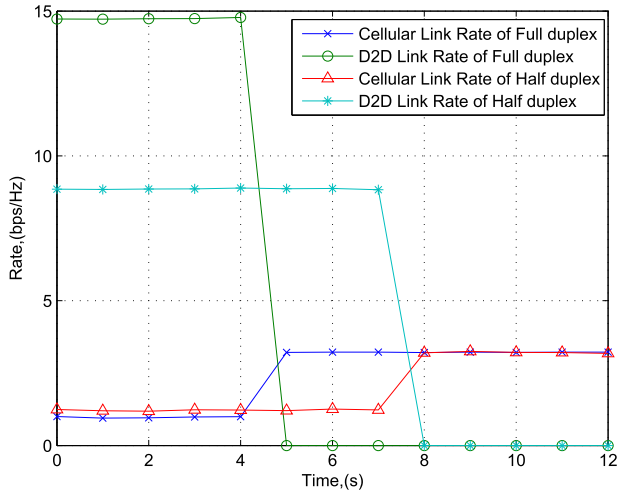

FIGURE 7. Performance gain comparison of HD-D2D and FD-D2D in terms of average link rate when a fixed-size data block is exchanged between each D2D pair.

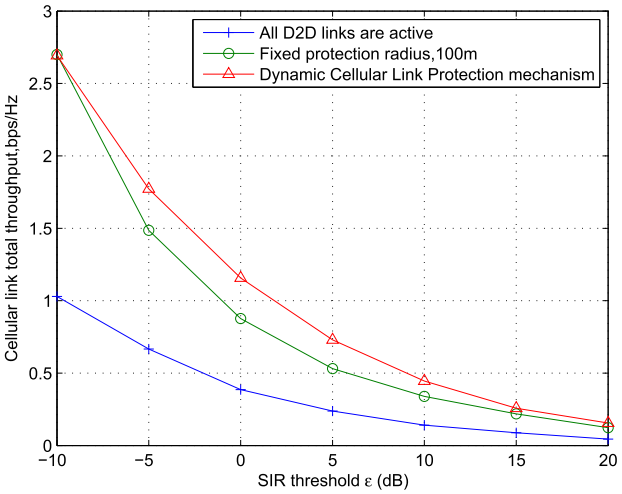

FIGURE 9. Cellular link performance in terms of sum throughput under three schemes: "all D2D links are activated", "fixed protecting-radius" and DCLP.

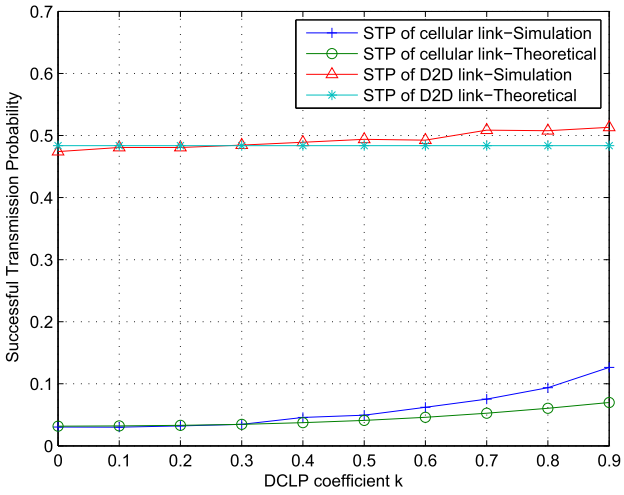

FIGURE 8. STP of cellular and D2D links with both theoretical approximation and simulation provided.

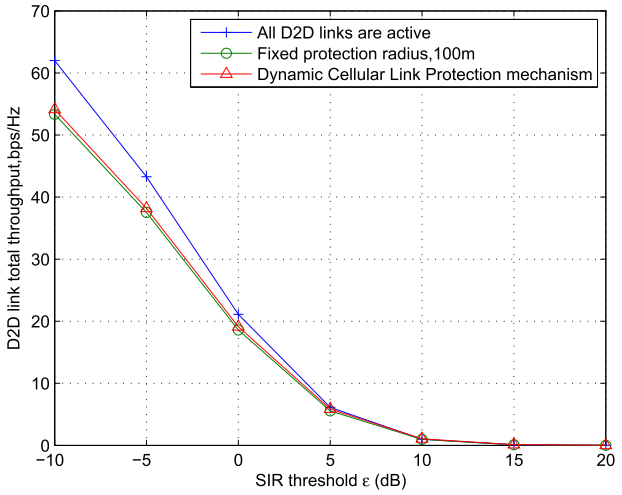

FIGURE 10. D2D link performance in terms of sum throughput under three schemes: "all D2D links are activated", "fixed protecting-radius" and DCLP.

average level of FD-D2D-induced interference imposed on the CUs is doubled compared with that induced by the HD-D2D mode). However, as an advantage, the FD-D2D mode is capable of completing the procedure of fixed-size-data exchange much quicker than the HD-D2D mode does, thus substantially shortening the interfering duration induced by activated FD-D2D links as compared with the latter. Consequently, in a statistical sense, the FD-D2D is likely to be more efficient than the HD-D2D in terms of the sum throughput of the whole underlaying network, despite of a much lower average interference imposed by the latter. As shown in Fig. 7, the area below the curve stands for the sum throughput during a D2D-active period, showing that the FD-D2D is capable of improving the sum throughput in consideration of the scenario of fixed-size-block exchange between D2D peers.

B. THE IMPACT OF THE DCLP MECHANISM

Under the proposed DCLP mechanism, the DUs located inside the BS-centric guard area of radius $R_p = k \cdot r$ are not allowed to transmit. As shown in Fig. 8, the STP may be impacted by variant settings of cellular-link-protecting-radius coefficient k according to the proposed DCLP mechanism. It is shown in Fig. 8 that the theoretical approximation derived in **Lemma 5** matches the simulation well, especially when the DCLP coefficient is lower than 0.7.

In Fig. 9 and Fig. 10, the sum throughput of cellular and D2D links will be compared by considering the following three schemes, i.e. *scheme #1*: all D2D links are activated, *scheme #2*: fixed protecting-radius, and *scheme #3*: DCLP mechanism). Both *scheme #2* and *scheme #3* are shown to be capable of improving the throughput of the cellular links. However, since some D2D links are inactivated in the above-mentioned two schemes, the throughput of D2D links will be eroded inevitably. Furthermore, an identical throughput at the D2D links can be obtained by employing *scheme #2* (with a fixed radius 100m considered) and *scheme #3*, with an

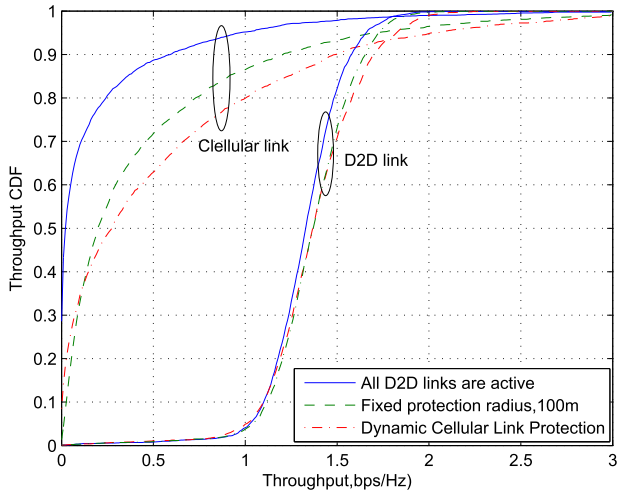

FIGURE 11. The distributions of average link throughput for cellular and D2D links under three schemes: "all D2D links are activated", "fixed protecting-radius" and DCLP.

additional gain in terms of cellular links' throughput obtained by employing the latter. The performance gains of *scheme #3* comes from the fact that the DCLP mechanism is able to adjust the protecting-radius dynamically according to the cellular links' instantaneous quality.

In Fig. 11, it compares the cumulative distribution functions (CDFs) of the average throughput in the cellular and D2D links. Since some D2D links will be inactivated when implement the DCLP mechanism, the D2D-induced interference can be substantially suppressed. Evidently, the DCLP mechanism is capable of facilitating a higher average throughput of both cellular and D2D links than *scheme #2*. Furthermore, the DCLP mechanism also shows the superiority over the *scheme #2* in terms of average link (i.e. with respect to both cellular and D2D links) throughput.

VI. CONCLUSION

In this paper, the benefits brought about by implementing FD-D2D mode in underlaying networks was analyzed. It was shown that the FD-D2D technique is capable of improving the throughput of the underlaying networks, provided that the SI power can be substantially reduced. Meanwhile, the tight bounds of throughput were derived. It was shown that the throughput of the underlaying network cannot be infinitely increased by simply increasing the density of DUs, and a break-even point appears once the interference has become the main factor restricting the performance of the system. Furthermore, to guarantee the quality of cellular links, we further proposed a DCLP mechanism to prevent the D2D links from being activated within the pre-set guard area. Numerical results showed that the proposed DCLP mechanism is capable of improving the cellular links' throughput without significantly eroding the throughput of the D2D links. In addition, it was also shown that the proposed DCLP mechanism is capable of providing a higher throughput than the "fixed protecting-radius" scheme does.

APPENDIX A

It is straightforward to derive the equations (5), (6), (8) and (9). In this section, we only focus on the derivations of (7) and (10). Based on the analysis of [36], the Laplace transforms of I_{dc} can be given by

$$\begin{aligned}
&\mathcal{L}_{I_{dc}}(s) \\
&= \mathbb{E}\left[\exp\left(-sP_d\sum_{\Phi_d}\left(h_{x_ib}d_{x_ib}^{-\alpha}+h_{m(x_i)b}d_{m(x_i)b}^{-\alpha}\right)\right)\right] \\
&= \mathbb{E}\left[\prod_{\Phi_d}\frac{1}{1+sP_d d_{x_ib}^{-\alpha}}\frac{1}{1+sP_d d_{m(x_i)b}^{-\alpha}}\right] \\
&= \exp\left[-2\pi\lambda_d\int_0^{\infty}\left(1-\frac{1}{1+sP_d x^{-\alpha}}\right.\right. \\
&\quad\left.\left.\times\frac{1}{1+sP_d\|x+D_d(\cos\varphi_i,\sin\varphi_i)\|^{-\alpha}}\right)x\mathrm{d}x\right] \\
&= \exp\left[-\lambda_d\int_0^{\infty}\left(2\pi-\frac{1}{1+P_d s x^{-\alpha}}f(s,D_d,\alpha)\right)x\mathrm{d}x\right],
\end{aligned} \tag{25}$$

where the last two steps are given out by changing the Cartesian integral to the polar integral. A similar derivation is employed in (10).

APPENDIX B

Since the closed-form expression is hard to obtain in resolving $f(s,D_d,\alpha)$, we need to derive the bounds of $\mathcal{L}_{I_{dc}}(s)$ and $\mathcal{L}_{I_{dd}}(s)$. From [36], the lower bound of $\mathcal{L}_{I_{dc}}(s)$ can be derived as

$$\begin{aligned}
\mathcal{L}_{I_{dc}}(s) &= \mathbb{E}\left[\prod_{\Phi_d}\frac{1}{1+sP_d d_{x_ib}^{-\alpha}}\frac{1}{1+sP_d d_{m(x_i)b}^{-\alpha}}\right] \\
&\geq \mathbb{E}\left(\prod_{\Phi_d}\frac{1}{1+sP_d d_{x_ib}^{-\alpha}}\right)\mathbb{E}\left(\prod_{\Phi_d}\frac{1}{1+sP_d d_{m(x_i)b}^{-\alpha}}\right) \\
&= \exp\left(-2\pi\lambda_d r^2\left(\frac{P_d}{P_c}\right)^{2/\alpha}\delta(\varepsilon,\alpha)\right),
\end{aligned} \tag{26}$$

in which the inequality follows the FKG inequality [34]. By combining (5), (6) and (26), after performing the integral, (11) can be derived.

The upper bound of $\mathcal{L}_{I_{dc}}(s)$ can then be given by

$$\begin{aligned}
&\mathcal{L}_{I_{dc}}(s) \\
&= \mathbb{E}\left[\prod_{\Phi_d}\frac{1}{1+sP_d d_{x_ib}^{-\alpha}}\frac{1}{1+sP_d d_{m(x_i)b}^{-\alpha}}\right] \\
&\leq \left[\mathbb{E}\left(\prod_{\Phi_d}\frac{1}{(1+sP_d d_{x_ib}^{-\alpha})^2}\right)\mathbb{E}\left(\prod_{\Phi_d}\frac{1}{(1+sP_d d_{m(x_i)b}^{-\alpha})^2}\right)\right]^{\frac{1}{2}} \\
&= \exp\left(-\left(1+\frac{2}{\alpha}\right)\pi\lambda_d r^2\left(\frac{P_d}{P_c}\right)^{2/\alpha}\delta(\varepsilon,\alpha)\right),
\end{aligned} \tag{27}$$

in which the inequality follows the Cauchy-Schwarz inequality. By combining (5), (6) and (27), after performing the integral, (12) can be derived.

APPENDIX C

For a typical cellular link, the hole of DUs can be classified into two groups, i.e. the nearest hole and the remainders. The reason for us to make this classification is that the receiver of interest (i.e. BS) is located inside the nearest hole (but outside the remainders). In other words, when the remainders are randomly distributed, the location of the nearest hole will act as the dominant role. Therefore, the holes must be treated differently.

Without loss of generality, we denote the nearest hole by $H_0(b_0, kr_0)$ and the remainders by $H_i(b_i, kr_i)$, $b_i \in \Phi_b$. The Laplace transforms of I_{dc}^n can be given by

$$
\begin{aligned}
&\mathcal{L}_{I_{dc}^n}(s)\\
&\overset{(a)}{=} \mathbb{E}\left[\exp\left(-sP_d \sum_{\Phi_d \setminus H_{0,i}} h_i d_i^{-\alpha}\right)\right]\\
&= \mathbb{E}\left[\exp\left(-sP_d\left(\sum_{\Phi_d \setminus H_0} h_i d_i^{-\alpha} - \sum_{b_i\in\Phi_b}\sum_{H_i} h_i d_i^{-\alpha}\right)\right)\right]\\
&\overset{(b)}{=} \exp\left[-\lambda_d \int_0^{\infty}\left(2\pi - \frac{f(s, D_d, \alpha)}{1 + P_d s x^{-\alpha}}\right) x \mathrm{d}x\right]\\
&\quad \times \mathbb{E}\left[\prod_{b_i\in\Phi_b} \exp\left(\int_{H_i} \frac{f(s, D_d, \alpha)}{1 + P_d s x^{-\alpha}} \mathrm{d}x\right)\right]\\
&\overset{(c)}{=} \exp\left[-\lambda_d \int_0^{\infty}\left(2\pi - \frac{f(s, D_d, \alpha)}{1 + P_d s x^{-\alpha}}\right) x \mathrm{d}x\right]\\
&\quad \times \mathbb{E}\Bigg[\prod_{b_i\in\Phi_b} \exp\Bigg(\int_{\|b_i\|-kr}^{\|b_i\|+kr} \frac{f(s, D_d, \alpha)}{1 + P_d s x^{-\alpha}}\\
&\quad \times \arccos\left(\frac{x^2 + \|b_i\|^2 - k^2 r^2}{2\|b_i\| x}\right) x \mathrm{d}x\Bigg)\Bigg]\\
&\overset{(d)}{=} \exp\left[-\lambda_d \int_0^{\infty}\left(2\pi - \frac{f(s, D_d, \alpha)}{1 + P_d s x^{-\alpha}}\right) x \mathrm{d}x\right]\\
&\quad \times \exp\left[-2\pi\lambda_b \int_{kr}^{\infty} (1 - e^{g(v,s)}) v \mathrm{d}v\right], \qquad (28)
\end{aligned}
$$

where in step (a), we have $h_i d_i^{-\alpha} = \left(h_{x_i b} d_{x_i b}^{-\alpha} + h_{m(x_i)b}\, d_{m(x_i)b}^{-\alpha}\right)$, and step (b) follows Appendix A. Note that the first term of step (b) denotes the area digging out the nearest hole, and its second term denotes the areas of other holes. Furthermore, step (c) is derived by replacing the Cartesian integral using the polar integral, and in (d), we can obtain the result $g(v, s) = \int_{v-kr}^{v+kr} 2\lambda_d \left(1 - \frac{f(s,D_d,\alpha)}{1+P_d s x^{-\alpha}}\right) \arccos\left(\frac{x^2+\|b_i\|^2-k^2r^2}{2\|b_i\|x}\right) x \mathrm{d}x$.

Acknowledgement

The authors would like to thank the anonymous reviewers for their critical comments, which greatly improved this paper.

REFERENCES

[1] Z. Zhang, K. Long, J. Wang, and F. Dressler, "On swarm intelligence inspired self-organized networking: Its bionic mechanisms, designing principles and optimization approaches," *IEEE Commun. Surveys Tuts.*, vol. 16, no. 1, pp. 513–537, Feb. 2014.
[2] S. Chen, F. Qin, B. Hu, X. Li, and Z. Chen, "User-centric ultra-dense networks for 5G: Challenges, methodologies, and directions," *IEEE Wireless Commun.*, vol. 23, no. 2, pp. 78–85, Apr. 2016.
[3] S. Chen and J. Zhao, "The requirements, challenges, and technologies for 5G of terrestrial mobile telecommunication," *IEEE Commun. Mag.*, vol. 52, no. 5, pp. 36–43, May 2014.
[4] Z. Zhang, K. Long, and J. Wang, "Self-organization paradigms and optimization approaches for cognitive radio technologies: A survey," *IEEE Wireless Commun.*, vol. 20, no. 2, pp. 36–42, Apr. 2013.
[5] C. Xing, Y. Ma, Y. Zhou, and F. Gao, "Transceiver optimization for multi-hop communications with per-antenna power constraints," *IEEE Trans. Signal Process.*, vol. 64, no. 6, pp. 1519–1534, Mar. 2016.
[6] Z. Liu, T. Peng, B. Peng, and W. Wang, "Sum-capacity of D2D and cellular hybrid networks over cooperation and non-cooperation," in *Proc. IEEE 7th Int. ICST Conf. Commun. Netw. China (CHINACOM)*, Aug. 2012, pp. 707–711.
[7] A. A. A. Haija and M. Vu, "Spectral efficiency and outage performance for hybrid D2D-infrastructure uplink cooperation," *IEEE Trans. Wireless Commun.*, vol. 14, no. 3, pp. 1183–1198, Mar. 2015.
[8] J. Liu, S. Zhang, H. Nishiyama, N. Kato, and J. Guo, "A stochastic geometry analysis of D2D overlaying multi-channel downlink cellular networks," in *Proc. IEEE Conf. Comput. Commun. (INFOCOM)*, May 2015, pp. 46–54.
[9] G. Fodor *et al.*, "Design aspects of network assisted device-to-device communications," *IEEE Commun. Mag.*, vol. 50, no. 3, pp. 170–177, Mar. 2012.
[10] L. Lei, Y. Kuang, X. Shen, C. Lin, and Z. Zhong, "Resource control in network assisted device-to-device communications: Solutions and challenges," *IEEE Commun. Mag.*, vol. 52, no. 6, pp. 108–117, Jun. 2014.
[11] D. Feng, L. Lu, Y. Yuan-Wu, G. Li, S. Li, and G. Feng, "Device-to-device communications in cellular networks," *IEEE Commun. Mag.*, vol. 52, no. 4, pp. 49–55, Apr. 2014.
[12] L. Wang, F. Tian, T. Svensson, D. Feng, M. Song, and S. Li, "Exploiting full duplex for device-to-device communications in heterogeneous networks," *IEEE Commun. Mag.*, vol. 53, no. 5, pp. 146–152, May 2015.
[13] Z. Zhang, K. Long, A. V. Vasilakos, and L. Hanzo, "Full-duplex wireless communications: Challenges, solutions, and future research directions," *Proc. IEEE*, vol. 104, no. 7, pp. 1369–1409, Jul. 2016.
[14] Z. Zhang, X. Chai, K. Long, A. V. Vasilakos, and L. Hanzo, "Full duplex techniques for 5G networks: Self-interference cancellation, protocol design, and relay selection," *IEEE Commun. Mag.*, vol. 53, no. 5, pp. 128–137, May 2015.
[15] B. Zhong and Z. Zhang, "Opportunistic two-way full-duplex relay selection in underlay cognitive networks," *IEEE Syst. J.*, vol. PP, no. 99, pp. 1–10, Jan. 2016.
[16] G. Zhang, P. Liu, K. Yang, Y. Du, and Y. J. Hu, "Orthogonal resource sharing scheme for device-to-device communication overlaying cellular networks: A cooperative relay based approach," *Sci. China Inf. Sci.*, vol. 58, no. 10, pp. 1–9, 2015.
[17] D. Feng, L. Lu, Y. Yuan-Wu, G. Y. Li, G. Feng, and S. Li, "Device-to-device communications underlaying cellular networks," *IEEE Trans. Commun.*, vol. 61, no. 8, pp. 3541–3551, Aug. 2013.
[18] G. Yu, L. Xu, D. Feng, R. Yin, G. Y. Li, and Y. Jiang, "Joint mode selection and resource allocation for device-to-device communications," *IEEE Trans. Commun.*, vol. 62, no. 11, pp. 3814–3824, Nov. 2014.
[19] X. Chai, X. Xu, and Z. S. Zhang, "A user-selected uplink power control algorithm in the two-tier femtocell network," *Sci. China Inf. Sci.*, vol. 58, no. 4, pp. 1–12, 2015.
[20] K. Doppler, C.-H. Yu, C. B. Ribeiro, and P. Janis, "Mode selection for device-to-device communication underlaying an LTE-advanced network," in *Proc. IEEE Wireless Commun. Netw. Conf. (WCNC)*, Apr. 2010, pp. 1–6.
[21] C.-H. Yu, K. Doppler, C. B. Ribeiro, and O. Tirkkonen, "Resource sharing optimization for device-to-device communication underlaying cellular networks," *IEEE Trans. Wireless Commun.*, vol. 10, no. 8, pp. 2752–2763, Aug. 2011.
[22] Y. Yang, Z. Liu, Z. Fu, T. Peng, and W. Wang, "Transmission capacity of device-to-device communication under heterogeneous networks with cellular users assisted," in *Proc. IEEE Globecom Workshops (GC Wkshps)* Dec. 2013, pp. 635–641.

[23] M. Belleschi, G. Fodor, and A. Abrardo, "Performance analysis of a distributed resource allocation scheme for D2D communications," in *Proc. IEEE GLOBECOM Workshops (GC Wkshps)*, Dec. 2011, pp. 358–362.
[24] S. Han, P. Chen, and C. Yang, "Full duplex assisted interference suppression for underlay device-to-device communications," in *Proc. IEEE Globecom Workshops (GC Wkshps)*, Dec. 2014, pp. 851–856.
[25] G. Zhang, K. Yang, P. Liu, and J. Wei, "Power allocation for full-duplex relaying based D2D communication underlaying cellular networks," *IEEE Trans. Veh. Technol.*, vol. 64, no. 10, pp. 4911–4916, Oct. 2015.
[26] H. Bagheri, F. A. M. Bonomi, and M. Katz, "Spectral efficiency and throughput enhancement by full-duplex D2D communication in mobile clouds," in *Proc. 21st Eur. Wireless Conf.*, May 2015, pp. 1–6.
[27] W. Cheng, X. Zhang, and H. Zhang, "Optimal power allocation for full-duplex D2D communications over wireless cellular networks," in *Proc. IEEE Global Commun. Conf. (GLOBECOM)*, Dec. 2014, pp. 4764–4769.
[28] Y. Zhou, H. Liu, Z. Pan, L. Tian, and J. Shi, "Energy efficient two-stage cooperative multicast: Effect of user density," *IEEE Trans. Veh. Technol.*, vol. 65, no. 9, pp. 7297–7307, Sep. 2016.
[29] J. Liu, H. Nishiyama, N. Kato, and J. Guo, "On the outage probability of device-to-device communication enabled multi-channel cellular networks: A RSS threshold-based perspective," *IEEE J. Sel. Areas Commun.*, vol. 34, no. 1, pp. 163–175, Jan. 2016.
[30] Q. Ye, M. Al-Shalash, C. Caramanis, and J. G. Andrews, "Distributed resource allocation in device-to-device enhanced cellular networks," *IEEE Trans. Commun.*, vol. 63, no. 2, pp. 441–454, Feb. 2015.
[31] V. Garcia, Y. Zhou, and J. Shi, "Coordinated multipoint transmission in dense cellular networks with user-centric adaptive clustering," *IEEE Trans. Wireless Commun.*, vol. 13, no. 8, pp. 4297–4308, Aug. 2014.
[32] *Study on LTE Device to Device Proximity Services, Radio Aspects Version 1.2.0*, document 3GPP TR36.843, 2014.
[33] X. Chai, Z. Zhang, and K. Long, "Joint spectrum-sharing and base station sleep model for improving energy efficiency of heterogeneous networks," *IEEE Syst. J.*, vol. PP, no. 99, pp. 1–11, Sep. 2015.
[34] S. N. Chiu, D. Stoyan, W. S. Kendall, and J. Mecke, *Stochastic Geometry and Its Applications*. New York, NY, USA: Wiley, 2013.
[35] Z. Yazdanshenasan, H. S. Dhillon, M. Afshang, and P. H. J. Chong. (2016). "Poisson hole process: Theory and applications to wireless networks." [Online]. Available: https://arxiv.org/abs/1601.01090
[36] Z. Tong and M. Haenggi, "Throughput analysis for full-duplex wireless networks with imperfect self-interference cancellation," *IEEE Trans. Commun.*, vol. 63, no. 11, pp. 4490–4500, Nov. 2015.

XIAOMENG CHAI received the B.Sc. degree in communication engineering from the University of Science and Technology Beijing (USTB), Beijing, China, , in 2012. He is currently pursuing the Ph.D. degree with the Institute of Advanced Network Technologies and New Services, USTB. His current research interests include heterogeneous networks, D2D communication, and resource optimization.

TONG LIU received the B.E. degree in automatic control from Harbin Engineering University (HEU) in 2000, the M.S. degree in navigation guidance and control from HEU in 2002, and the Ph.D. degree in electrical engineering from the Harbin Institute of Technology in 2006. In 2006, he joined Huawei Technologies Ltd., as an Associate Researcher. He is currently an Associate Professor with the School of Information and Communication Engineering, HEU. His main research interests include tactical networking and software-defined radio.

CHENGWEN XING received the B.Eng. degree from Xidian University, Xi'an, China, in 2005 and the Ph.D. degree from the Department of Electrical and Electronic Engineering, The University of Hong Kong, Hong Kong, in 2010. Since 2010, he has been with the School of Information and Electronics, Beijing Institute of Technology, Beijing, China, where he is currently an Associate Professor. His current research interests include statistical signal processing, convex optimization, multivariate statistics, combinatorial optimization, and cooperative communication systems.

HAILIN XIAO was born in 1976. He received the B.S. from Wuhan University in 1998, the M.S. degree from Guangxi Normal University in 2004, and the Ph.D. degree from the University of Electronic Science and Technology of China in 2007. He was a Professor with the School of Information and Communications, Guilin University of Electronic Technology. He is currently a Research Fellow with the Joint Research Institute for Signal and Image Processing, School of Engineering and Physical Sciences, Heriot-Watt University. His research interests include MIMO wireless communications, cooperative communications, and smart antenna techniques.

ZHONGSHAN ZHANG received the B.E. and M.S. degrees in computer science from the Beijing University of Post and Telecommunications (BUPT) in 1998 and 2001, respectively, and the Ph.D. degree in electrical engineering from BUPT in 2004. From 2004, he joined the DoCoMo Beijing Laboratories as an Associate Researcher, and was promoted to be a Researcher in 2005. In 2006, he joined the University of Alberta, Edmonton, AB, Canada, as a Post-Doctoral Fellow. In 2009, he joined the Department of Research and Innovation, Alcatel-Lucent, Shanghai, as a Research Scientist. From 2010 to 2011, he was with the NEC China Laboratories, as a Senior Researcher. He is currently a Professor with the School of Computer and Communication Engineering, University of Science and Technology Beijing. His main research interests include statistical signal processing, self-organized networking, cognitive radio, and cooperative communications. He served or is serving as a Guest Editor and/or an Editor for several technical journals, such as the *IEEE Communications Magazine* and the *KSII Transactions on Internet and Information Systems*.